



Contents lists available at SciVerse ScienceDirect

Journal of Great Lakes Research

journal homepage: www.elsevier.com/locate/jglr

Evolution of a cyanobacterial bloom forecast system in western Lake Erie: Development and initial evaluation

Timothy T. Wynne^{a,*}, Richard P. Stumpf^a, Michelle C. Tomlinson^a, Gary L. Fahnenstiel^b, Julianne Dyble^c, David J. Schwab^c, Sonia Joseph Joshi^d

^a NOAA, National Centers for Coastal Ocean Science, 1305 East-West Highway, Silver Spring, MD 20910, USA

^b NOAA, Great Lakes Environmental Research Laboratory, Lake Michigan Field Station, 1431 Beach Street, Muskegon, MI 49441, USA

^c NOAA, Great Lakes Environmental Research Laboratory, 4840 South State Road, Ann Arbor, MI 48108, USA

^d NOAA, Michigan Sea Grant Extension/NOAA Center of Excellence for Great Lakes and Human Health, 4840 South State Road, Ann Arbor, MI 48108, USA

ARTICLE INFO

Article history:

Received 17 October 2011

Accepted 23 October 2012

Available online xxxx

Communicated by Robert Shuchman

Keywords:

Remote sensing

Cyanobacteria

Ecological forecasting

Lake Erie

Microcystis

Optics

ABSTRACT

In the summer of 2008 the National Oceanic and Atmospheric Administration began monitoring cyanobacterial blooms in Lake Erie using high temporal resolution satellite imagery. In 2009, a forecast of bloom transport was also developed using a hydrodynamic model to forecast the trajectory of the bloom. These forecasts have been disseminated from 2008 to the present in the form of a bulletin which is emailed to local managers, health departments, researchers and other stakeholders. The number of bulletins issued each year, as well as the number of subscribers that receive the weekly bulletins, has increased significantly every year that the system has been in place. This manuscript discusses results from the first 3 years that the forecasts were distributed (2008–2010), describes the components of the forecasts, and will conclude with possible improvements that could be made to the forecast system. Harmful algal blooms of the genus *Microcystis* were found in all 3 years, and the development of these blooms was associated with water temperatures $> 18^{\circ}\text{C}$ and wind stresses $< 0.04\text{ Pa}$. Wind stresses $> 0.1\text{ Pa}$ were associated with bloom dispersment as were temperatures $< 18^{\circ}\text{C}$. The present forecasting system was deemed adequate, but improvements in the use of additional remote sensing products and post-processing would yield a more accurate forecast.

Published by Elsevier B.V. on behalf of International Association for Great Lakes Research.

Introduction

Lake Erie, particularly the shallow, nutrient enriched western basin, has recurring summer blooms of toxic cyanobacteria primarily of the genera *Microcystis* (Rinta-Kanto et al., 2005). Nutrient over-enrichment resulted in massive cyanobacterial blooms in western Lake Erie during the 1960s and 1970s, but the implementation of phosphorus abatement strategies in the 1980s was effective in significantly reducing cyanobacterial blooms in the lake until the mid-1990s (Makarewicz, 1993). In the mid-1990s invasive zebra mussels (*Dreissena polymorpha*) colonized western Lake Erie and, shortly after their arrival, the resurgence of cyanobacterial blooms was noted (Nicholls and Hopkins, 1993). It has been hypothesized that this is a result of the zebra mussels increasing water clarity and selectively preying on eukaryotic phytoplankton (Budd et al., 2001; Juhel et al., 2006; Vanderploeg et al., 2001).

The dominant bloom forming cyanobacteria in Lake Erie, *Microcystis aeruginosa*, produces the hepatotoxin microcystin which has been documented to cause mortalities in wild and domestic animals and sicken

people (Falconer, 2005; Fleming et al., 2002). In this manuscript, a bloom is considered high biomass of a singular species (rather than a rapid growth), which is loosely adapted from a definition from Richardson (1989) and from Smayda (1997). Preliminarily *Microcystis* concentrations in the range of 35,000 cells mL^{-1} were adequately detected with remote sensing (Wynne et al., 2010). The World Health Organization (WHO) has set preliminary guidelines for microcystin concentrations in drinking water of $1\text{ }\mu\text{g L}^{-1}$, and $20\text{ }\mu\text{g L}^{-1}$ for recreational exposure (WHO, 2003), and 105 cells mL^{-1} is considered a threshold for potential risk (Graham et al., 2009). Other cyanobacteria in the Great Lakes are also capable of producing toxins, including *Anabaena circinalis*, *Anabaena flos-aquae*, *Aphanizomenon flos-aquae*, and *Cylindrospermopsis raciborskii*. In addition to the potential toxicity, cyanobacterial blooms can form surface scums that reduce the aesthetics of recreational waters and produce chemical compounds that cause taste and odor issues in municipal drinking waters (Paerl et al., 2001). This problem is further exacerbated by the tendency of a bloom to be concentrated by wind in harbors, shorelines, docks and other near shore areas where they are more likely to be encountered by the public (Ibelings et al., 2003).

By disseminating a nowcast (a computer generated estimate of where the bloom is at the time the forecast is issued) and a forecast (an estimate of where the bloom is likely to be going within the

* Corresponding author at: 1305 East-West Highway Silver Spring, MD 20910, USA. Tel.: +1 301 713 3028.

E-mail address: timothy.wynne@noaa.gov (T.T. Wynne).

next 3 days), natural resource and public health managers are better prepared to make necessary arrangements to mitigate any detrimental impacts that these blooms may cause. Municipal water managers may be able to use the forecast to alleviate taste and odor issues that are associated with cyanobacterial blooms. Beach managers may also be able to utilize the forecasts as a tool to post-warnings to the public near beaches that are affected, or that are forecasted to be affected. Interested members of the scientific research community also subscribe to the forecast system as it may help target their own research as well as providing validation of the satellite imagery used in the forecast system.

The National Oceanic and Atmospheric Administration (NOAA) started producing forecasts that monitor the abundance and forecast the transport of Harmful Algal Blooms (HABs) in the Gulf of Mexico in 2000; these became operational in 2004 as the NOAA Harmful Algal Bloom Forecasting System (NOAA HAB-FS). The forecasts are currently being made for the toxic dinoflagellate *Karenia brevis*, although the presence of additional harmful phytoplankton assemblages (e.g. *Dinophysis* spp.) and benign algal bloom species (e.g. *Trichodesmium* spp.) are also noted. These forecasts are produced through NOAA's Center for Operational Oceanographic Products and Services (CO-OPS) and in 2010 CO-OPS began operational forecasts for the toxic dinoflagellate, *Karenia brevis*, in the western Gulf of Mexico. NOAA (2008) has defined operational as: "sustained, systematic, reliable, and robust mission activities with an institutional commitment to deliver appropriate, cost-effective products and services". CO-OPS issued forecasts are delivered biweekly and are made using standardized protocols, thorough documentation of the forecast system and a reliable, quality controlled and backed-up forecast system. Methods and details of NOAA's operational HAB forecast system can be found in Stumpf et al. (2003); Tomlinson et al. (2004); Wynne et al. (2005); Fisher et al. (2006); and Stumpf et al. (2009). Other regions of the US will be added to the HAB-FS based on funding and need, with western Lake Erie being the next probable area included. Since 2008 the HAB-FS has been in an experimental mode for *Microcystis* blooms in western Lake Erie, with improvements being made every year. We here describe the plan to move these forecasting strategies from a research and development capacity into a fully operational mode.

Methods

Satellite imagery

The forecast system uses high temporal resolution imagery from the Medium Resolution Imaging Spectrometer (MERIS) on board the European Space Agency satellite, Envisat-1. This sensor provides data several (~4–5) times per week at the latitude of Lake Erie. As a general rule at least half of these images will be obscured by clouds making them useless or only moderately useful depending on the amount of clouds present in the scene. MERIS comes in two spatial resolutions, a Full Resolution (FR) image with a 260 m × 300 m pixel size, and a Reduced Resolution (RR) image at 1040 m × 1200 m pixel size (ESA, 2012). The size of these pixels will make very small features and sub pixel variability a potential issue; however previous experience suggests that major features like large cyanobacterial blooms in a sizeable catchment such as western Lake Erie should not present a significant impediment the majority of the time. An example of the differences in satellite resolution can be seen in Fig. 1.

For the 2008 and 2009 forecast years, standard Level-2 (L2) RR imagery was acquired from the European Space Agency (Montagner, 2001). Based on feedback from the user community, it was decided that the system should switch to the Full Resolution imagery in 2010. Level-1 Full resolution MERIS imagery became routinely available in early 2009 by Canada Centre for Remote Sensing receiving stations in Gatineau and Prince Albert, Canada and was obtained

through the National Aeronautics and Space Administration (NASA) ocean biology processing group (<http://oceancolor.gsfc.nasa.gov/>). The imagery was processed through the Naval Research Laboratory's Automated Processing System (APS), which uses the NASA Level 2 generation (l2gen) software package. This processing scheme presented an unexpected challenge. Near the summer solstice the sun angle is such that it causes somewhat severe sun glint to contaminate the imagery. The change in processing with the use of the FR data in 2010 led to the use of a threshold cloud masking procedure. The threshold cloud mask was satisfactory in the early spring tests when sun glint was absent, but masked glint areas as clouds in summer. (The ESA cloud mask included in the RR image products has corrections to compensate for glint.) Since the algorithms for locating cyanobacterial blooms deliver satisfactory results in areas affected by sun glint and the sensor was still able to retrieve reliable data despite the sun glint, no cloud mask was used for the majority of the forecasts issued in 2010 to avoid masking measurable data. This resulted in areas under clouds assigned the designation as "non-bloom" regardless if there was a bloom present in that area. When this was the case the analysts who issued the forecasts made every effort to note this within the written text of the forecasts. After 2010, the cloud mask algorithm for the FR was modified to separate glint and clouds.

Once the imagery was processed to normalized surface reflectance (reflec) using methods described by Montagner (2001), the cyanobacteria index (CI) was calculated as:

$$CI = -SS(681) \quad (1)$$

Where the spectral shape (or curvature) was determined as

$$SS(\lambda) = \text{reflec}(\lambda) - \text{reflec}(\lambda^-) - \left\{ \text{reflec}(\lambda^+) - \text{reflec}(\lambda^-) \right\} \times \frac{(\lambda - \lambda^-)}{(\lambda^+ - \lambda^-)} \quad (2)$$

where $\lambda = 681$ nm (MERIS band 8), $\lambda^+ = 709$ nm (band 9), and $\lambda^- = 665$ nm (band 7). This algorithm was first introduced as a cyanobacterial detection algorithm in Lake Erie by Wynne et al., 2008 and later renamed CI and applied in Wynne et al. (2010) and Wynne et al. (2011). The normalized water reflectance (ESA L2 data) was used for reflec in 2008 and 2009, but in 2010, as well as in the future when MERIS FR imagery is available; the l2gen Rayleigh scattering corrected surface reflectance (ρ_{rs}) (NASA, 2011) was used in place of reflec. Details of the algorithm are beyond the scope of this publication and the interested reader is encouraged to consult these previous publications for additional details.

Ancillary data

Ancillary data, including wind speed and water temperature, is collected from the buoys operated by the National Data Buoy Center (NDBC). Data from multiple NDBC buoys may be used, depending on which ones are closer to a feature of interest or actively collecting data during the time period of interest. Data from only one buoy is shown on each forecast for simplicity. These blooms have a tendency to be large (covering hundreds to thousands of square kilometers), and the conditions at the chosen buoy will not necessarily be identical to locations throughout western Lake Erie, but the data should trend the same way. Commonly used buoys are: Toledo Light No. 2 (THLO1), station 45005, Marblehead (MRHO1), and South Bass Island (SBO1) (Fig. 2). NDBC data are acquired and averaged into daily increments; defining a day as the 24 h preceding 10:00 EST. MERIS collects data approximately 10:30 AM EST (Rast et al., 1999) so this spatial averaging method shows the average conditions for the 24 h period just before image acquisition. Wind speed was used to

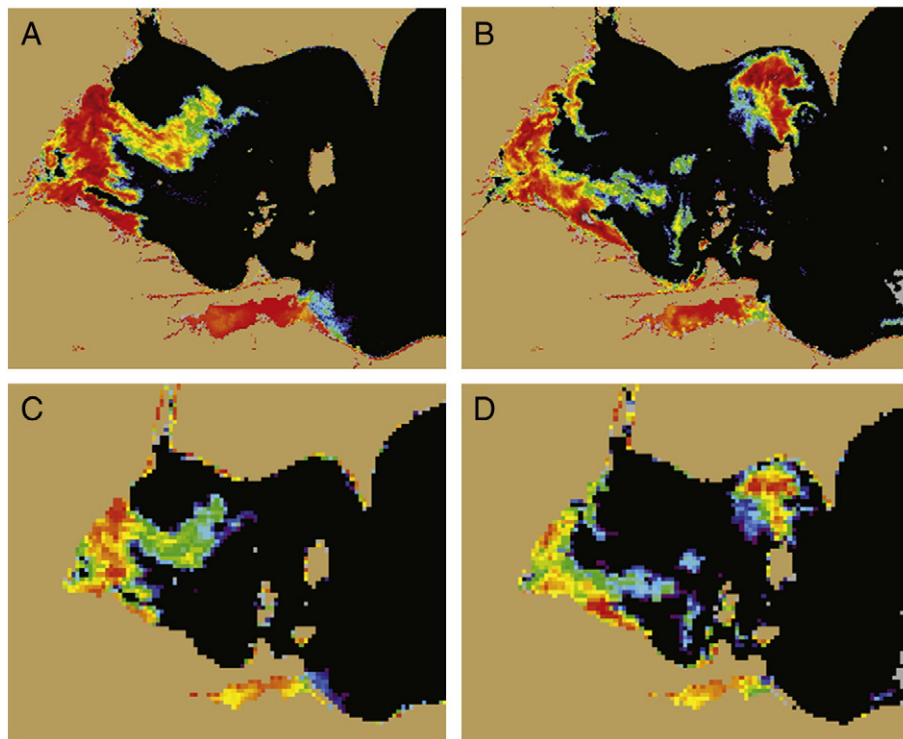


Fig. 1. Imagery illustrating the differences between MERIS RR and FR pixels. An FR image from 13 September 2010 (A), an FR image from 29 September 2010 (B), an RR image from 13 September 2010 (C) and an RR image from 29 September 2010 (D) are compared.

calculate wind stress by methods shown by Hsu (1973). The wind stress and water temperature is then graphically depicted in the bulletin.

Hydrodynamic model

The modeling system is discussed in detail in Wynne et al. (2011). The components are described here. A hydrodynamic model was

incorporated into the system as a means of determining the likely transport of the bloom feature identified from the satellite imagery. The hydrodynamic model chosen was the Great Lakes Coastal Forecasting System (GLCFS, Schwab and Bedford, 1999). The model is run for all five of the Laurentian Great Lakes, allowing simulation techniques described here to be potentially transferable to other parts of the Great Lakes. This model is also scheduled to become operational in CO-OPS within the next 1–2 years, replacing the current version. The model is

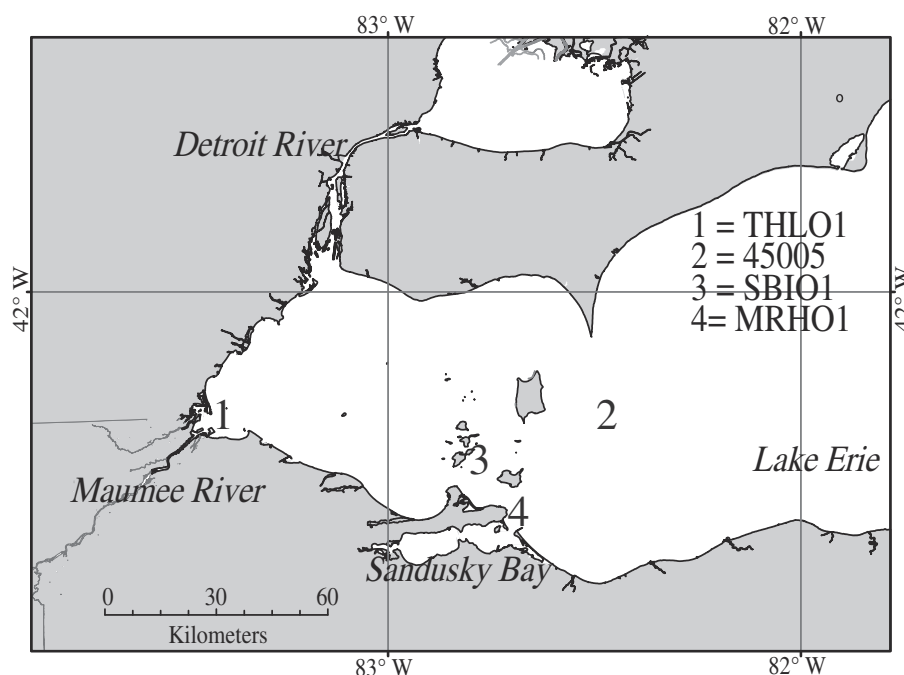


Fig. 2. A map of the study area. Numbers denote the location of National Data Buoy Center (NDBC) buoys. THLO1 is Toledo Light No 2, 45005 is station 45005, MRHO1 is Marblehead and SBIO1 is South Bass Island.

run in real time and is updated every 6 h, with observed wind replacing forecasted wind in 6-h increments. Outputs of the model are saved every hour. Every 12 h, a model run is made using wind forecasts from the National Centers for Environmental Prediction (NCEP) which results in current forecasts for up to 5 days beyond the present.

Particle tracking

A particle tracker is used in this forecast system as a way to combine the feature detected and delimited from the satellite imagery with a hydrodynamic model, in order to approximate the likely trajectory of the bloom feature. The particle tracker employed here is the General NOAA Operational Modeling Environment (GNOME). The input for GNOME is a file which contains the hydrodynamic model to be run and a file with a series of points in it, called Lagrangian Elements (LE), which are derived from the satellite imagery. Each pixel in the imagery that possesses a positive CI (i.e. any pixel flagged as likely representing a cyanobacterial bloom) has its CI multiplied by a constant in order to assign a number of points to be moved in space and time by the particle tracker. The model runs required a balance between the total number of particles and the number of particles allocated in each pixel. A multiplier of 5,000 produced approximately 25 points per pixel in areas with high bloom concentrations (high CI), and was determined to produce an adequate number of LE points to be present for a representative simulation. These points were randomly distributed within the space of each pixel. The FR imagery

has 16 times the number of pixels and thus runs much slower than the RR, but all simulations are generally done in under an hour.

Once the LEs are loaded into GNOME they are simulated forward in time using input modeled surface currents from the GLCFS. The simulation is stopped at two times during the run and the LEs are written back out into two images which represent a nowcast and a forecast. Typically the image being used is at least 24 h old. The satellite data sets are usually available between 20 and 30 h after collection, with a few hours needed for post-processing. The most recent usable image is used; this may be several days old. As same day imagery is not available for the forecast, a nowcast is required—the nowcast being the simulation between image acquisition time and the morning of the simulation run. The GLCFS uses observational data to create a hindcast. The hindcast currents are used to create the nowcast from GNOME. The GLCFS runs a 120 h forecast. The forecast modeled data is used to project the nowcast into the future to create a forecast. For additional information on the techniques and examples used in the modeling for this forecasting system consult Wynne et al. (2011).

Bloom statistics

Bloom characteristics were evaluated on a post hoc basis after the conclusion of a bloom season to determine bloom intensity and bloom area. The intensity was derived by taking a cumulative sum of all pixels with a positive CI. This number was then normalized by

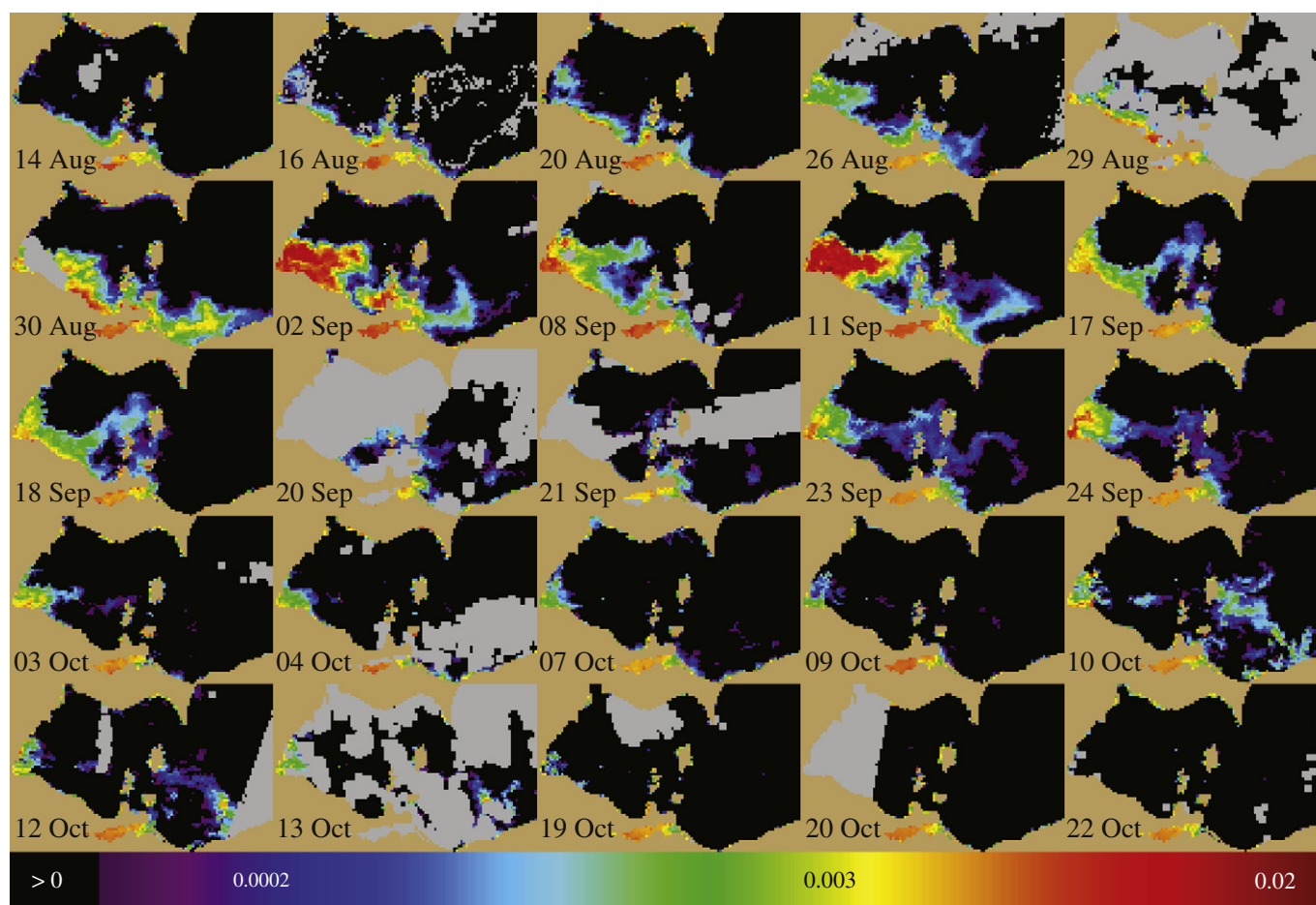


Fig. 3. A time series of MERIS derived cyanobacterial index imagery from 2008. Black is indicative of pixels with a very low likelihood of a bloom, gray indicates clouds or missing data (off-nadir), and colored pixels are probable locations of cyanobacterial blooms. Warmer colors (red, orange, and yellow) are indicative of high concentrations of cyanobacteria and cooler colors (blue and purple) are indicative of low concentrations. Units are expressed in $\text{mW}/\text{cm}^2/\mu\text{m}/\text{sr}$. This figure was previously published (Wynne et al., 2010; Copyright (2010) by the Association for the Sciences of Limnology and Oceanography, Inc.). (For interpretation of the references to color in this figure legend, the reader is referred to the web version of this article.)

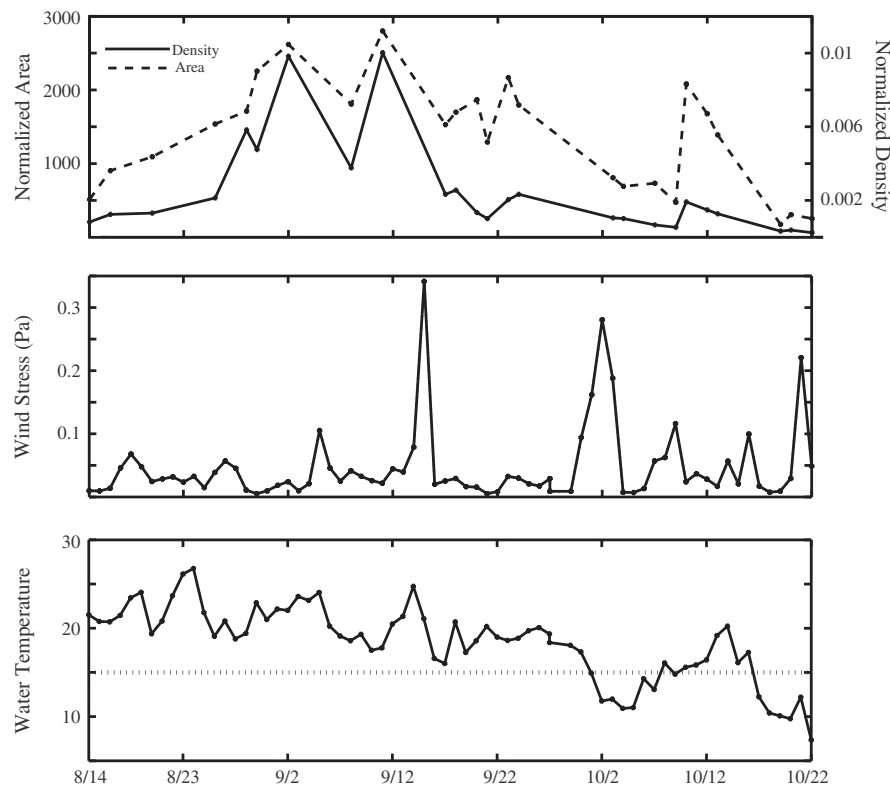


Fig. 4. Time series plots from 14 August to 22 October 2008. (A) Graph showing the normalized areal coverage of the bloom (dashed line) and the normalized density of the bloom (solid line). This data was extracted from the time series in Fig. 3. Note that the two lines closely follow each other in shape and magnitude until the large wind event on 15 September, after which the shapes are still similar but the density is much reduced. (B) Graph showing the mean daily wind stress from wind speed data reported by NOAA's NDBC station 45005. (C) Graph showing the mean daily water temperature as reported by NOAA's CO-OPS station at 45005. The dashed line shows the 15 °C point mentioned in the text.

the number of clear pixels from the region that included all pixels that exhibited a positive CI during any image for the bloom season. Likewise the area of the bloom was calculated by adding the number of pixels with a positive CI at any point during the time series and normalized in the same fashion.

Results and discussion

Summary of 2008 season

In 2008 the cyanobacterial detection algorithm was first applied to the near real time imagery (Fig. 3) and the corresponding wind stress and water temperatures were plotted as well as a graphical representation of the bloom area and intensity (Fig. 4). The analysis in 2008 did not include the forecasted positions. It was done as a “proof of concept” and distributed to a handful of users. The results of this year were summarized in Wynne et al., 2010. The bloom was a relatively intense bloom and persisted for about 70 days between 14 August and 22 October, which is the latest starting bloom of the 3 years considered here.

Summary of 2009 season

In 2009 forecasts were introduced as products and the bulletins were made on a more regular basis. In all, 13 weekly bulletins were made from 23 July, which coincides with the first feature consistent with a bloom, to 15 October, when it was concluded that no significant levels of cyanobacteria were present. The satellite imagery for this time series is shown in Fig. 5 with the ancillary data in Fig. 6. The imagery does not detect any bloom features on 7 July, but by 14 July a feature began to develop in the western basin of Lake Erie and slowly grew until 5 August (Fig. 7). Between 5 August and 14 August, the feature began a period of relatively rapid expansion and then went through a

period of decline between 15 August and 24 August. The wind stress during this time period spiked on 20–21 August (Fig. 6). Unfortunately the imagery from this period was contaminated with clouds, and was relatively poor as a result. Seemingly the bloom started a period of rapid expansion following the high wind events of August 21 and 22. Following these high wind events, the 24 August image suggests a relatively high biomass bloom although much of the imagery during this period is masked by clouds. The high bloom biomass during this period is accompanied by low wind stress and warm water temperatures, conditions favoring bloom maintenance, growth and increased buoyancy. From 30 August through 1 September there was a large wind event which brought about mixing that reduced the surface biomass, as seen in the image from 31 August. This wind event corresponded to a steep decline in water temperature (Fig. 6), on the order of 4 °C in the span of 3 days. By 5 September the satellite data indicated that the bloom was at its maximum concentration. The bloom appeared to contract from 5 September through 9 September, which may be tied to a mild wind event (~0.11 Pa). After 9 September the bloom once again showed a dramatic increase in surface biomass, rebounding to similar intensities as were seen in the 5 September image. This change is consistent with buoyancy during low wind stress (Wynne et al., 2010) rather than nutrient influx, as *M. aeruginosa* is relatively slow growing, with growth reported to be on the order of 0.1 day⁻¹ (Fahnenstiel et al., 2008). The image was cut off and is at the edge of the scene, so the eastern most portion of the feature is obstructed. After 11 September the bloom slowly began to dissipate with more frequent wind events and a decreasing water temperature and no feature indicative of a cyanobacterial bloom was detected after 10 October.

Summary of 2010 season

In 2010 the bulletin was further standardized to be issued starting on the predetermined date of 1 June instead of when a potential

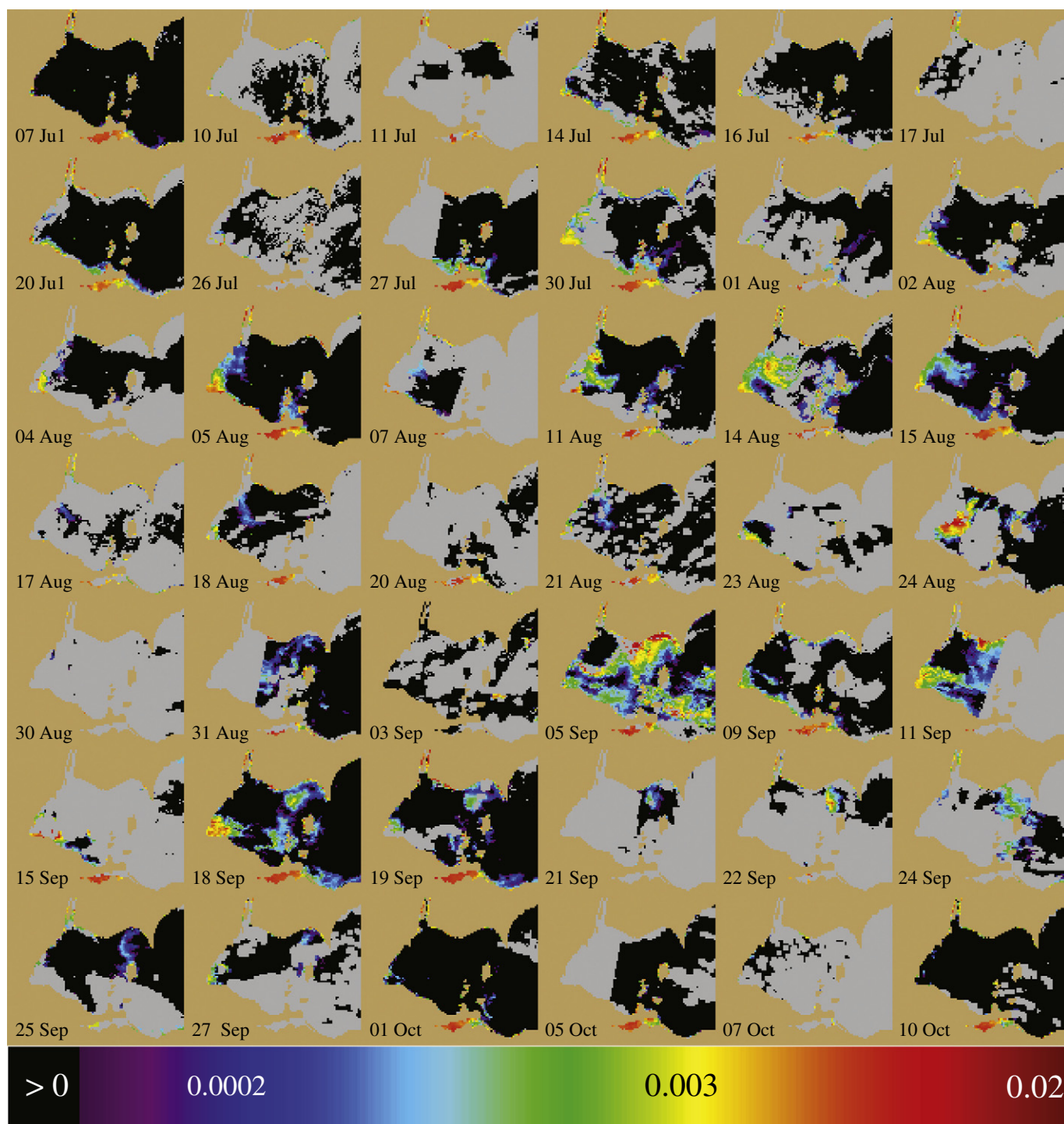


Fig. 5. A time series of MERIS derived cyanobacterial index imagery from 2009. See Fig. 3 caption for additional details.

bloom feature was present in the imagery. Cyanobacterial blooms are thought to be uncommon but possible in early June in Lake Erie. The bulletin was issued weekly until the end of the bloom season when bloom features were no longer present in the imagery. There was 1 week where no bulletin was issued due to lack of staff, which further illustrates the need to move the forecasting out of a Research and Development program and into a fully operational environment. Fig. 7 shows the imagery from the 2010 bloom, and Fig. 8 shows the corresponding ancillary data.

A feature flagged as a cyanobacterial bloom appeared in the imagery on 25 June 2010. This feature was slightly smaller on 29

June, and then started to expand for several consecutive images, spanning approximately 1 week. Sampling revealed that the bloom was comprised of the chlorophyte *Pandorina* and not *Microcystis*. This highlights the need for validation of remotely sensed features. The *Pandorina* bloom appeared to have dissipated by 17 July, when no feature was present in the imagery that indicated a bloom.

By 27 July another feature was present in the imagery. This was confirmed by field samples as *Microcystis aeruginosa*. The feature maintained a relatively low concentration and density until 7 September, when the bloom started to expand fairly rapidly, and

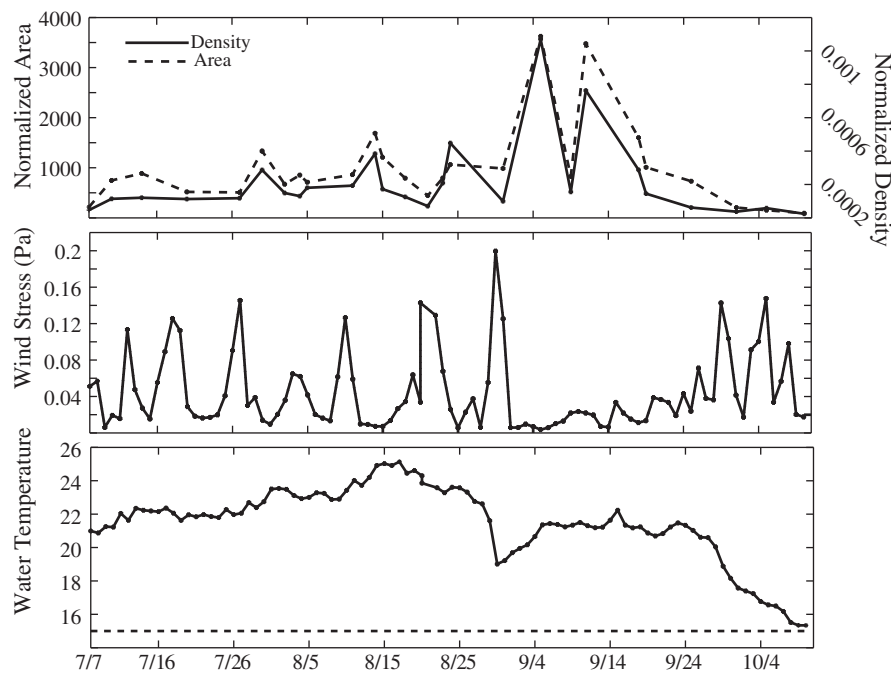


Fig. 6. Time series plots from 7 August to 10 October 2009. (A) Graph showing the normalized areal coverage of the bloom (dashed line) and the normalized density of the bloom (solid line). This data was extracted from the time series in Fig. 6. (B) Graph showing the mean daily wind stress from wind speed data reported by NOAA's NDBC station 45005. (C) Graph showing the mean daily water temperature as reported by NOAA's CO-OPS station at 45005. The dashed line shows the 15 °C point mentioned in the text.

continued to grow until 23 September, where it reached its peak density and concentration. On 15 September a surface cyanobacterial surface scum was noted, which was confirmed by field sampling to be dominated by *Anabaena* spp., with smaller concentrations of *M. aeruginosa* intermixed (T. Bridgeman, unpublished data). While nutrient data was not yet available at the time of this writing, it is hypothesized that the *M. aeruginosa* bloom drove western Lake Erie to nitrogen limitation and this favored the nitrogen-fixing cyanobacteria of the genera *Anabaena*. In nitrogen limiting conditions *Anabaena* spp., has a competitive advantage over *M. aeruginosa*. While blooms of *Aphanizomenon* spp. have been noted regularly to succeed *M. aeruginosa* in western Lake Erie, it is thought that *Anabaena* succession is relatively rare (T. Bridgeman, personnel communication). The bloom disappeared from the imagery by 12 October.

Design of bulletin

For maximum effectiveness per unit effort it was determined that the forecasts should be issued as an Adobe Portable Document File (pdf), no more than 2 pages in length. This conclusion was supported by meeting with coastal resource managers. It allows the forecasts to be rapidly distributed to a large number of users using little computational resources on the end of the subscribers. The forecasts of the cyanobacterial bloom detection system were based on a similar system developed by Stumpf et al. (2003), which forecasted blooms of the harmful dinoflagellate *Karenia brevis* in the Gulf of Mexico. These forecasts have been issued since 2004 and user feedback favored this format. In addition, some of the management community prefers Geographic Information System (GIS) compatible formats for the imagery, such as geoTIFFS, which are routinely produced and available upon request.

A typical bulletin consists of two pages. The first page shows the imagery from the Cyanobacterial Index (Supplementary Online Information Fig. 1). The first image on page 1 of the bulletin is the MERIS image from the sampling date or the most recent image available. The second image is the nowcast, defined as the estimated location of the cyanobacterial bloom at the time that the

bulletin is issued. Since the most recent image is generally is at least 24 h old, due to time needed for data acquisition and processing, the feature is simulated forward in time to show the likely position of the bloom at the present. The nowcast is made using the GLCFS model but the model is run using observational meteorological data, as opposed to forecasted data, theoretically making the nowcast simulation more reliable than a forecast. The third and final image on page 1 of the bulletin is the forecasted location, which is generally projected 72 h forward from the time of the nowcast image.

Water temperature and wind stress preceding and during the bloom as recorded at the appropriate buoys is given on page 2 of the bulletin (Supplemental Online Information Fig. 1). These factors are considered critical in the formation and maintenance of cyanobacterial blooms (Paerl, 1988; Paerl and Huisman, 2008; and Sellner, 1997). Wynne et al. (2010) indicate that *Microcystis* spp. blooms in Western Lake Erie had a tendency to rapidly dissipate when the water temperature dropped below 15 °C. Data presented here from the 2009 and 2010 bloom season does not necessarily support this hypothesis. While it appears that blooms dissipate during rapidly falling temperatures these changes are also associated with more frequent wind events (Fig. 6). It has been suggested that wind stress plays a major role within the vertical distribution of the cyanobacterial bloom (Hunter et al., 2008; Wynne et al., 2010, 2011). The buoyancy of *Microcystis* cells will result in the formation of a surface scum in the absence of strong wind events, which will be readily detected by satellite imagery. However, Wynne et al. (2010) suggested that a wind stress exceeding 0.1 Pa is capable of mixing the bloom more or less homogeneously throughout the water column, resulting in a significant reduction in the biomass in the surface layer (less than 1 m) that will be visible in the imagery. As a result the bloom will look like it went through a major period of subsidence during this time period, when in fact the bloom had not lost any significant biomass, but just changed in vertical distribution. Therefore, to better interpret bloom dynamics and accurately forecast bloom events, it is necessary to look at both water temperature and wind stress.

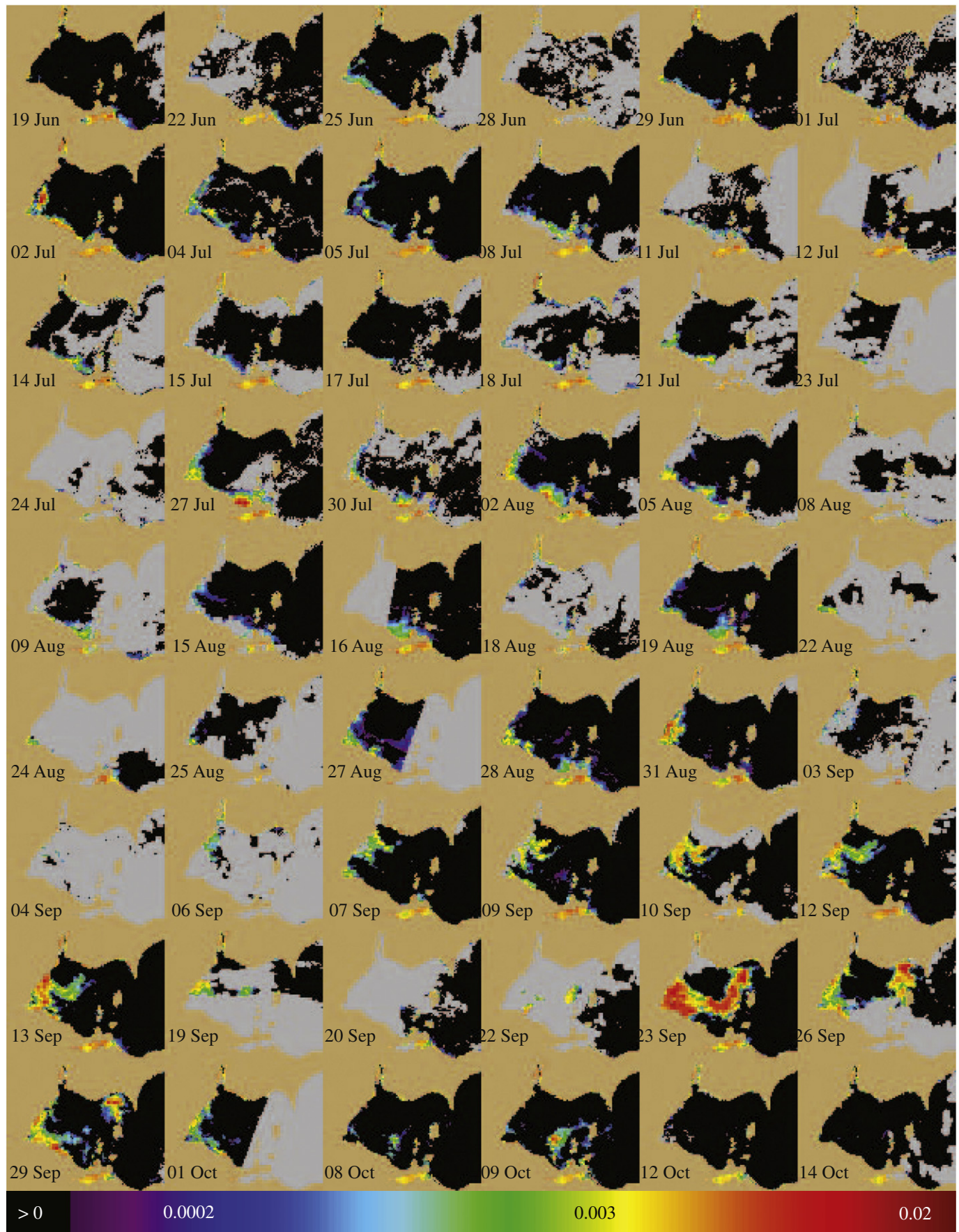


Fig. 7. A time series of MERIS derived cyanobacterial index imagery from 2010. See Fig. 3 caption for additional details.

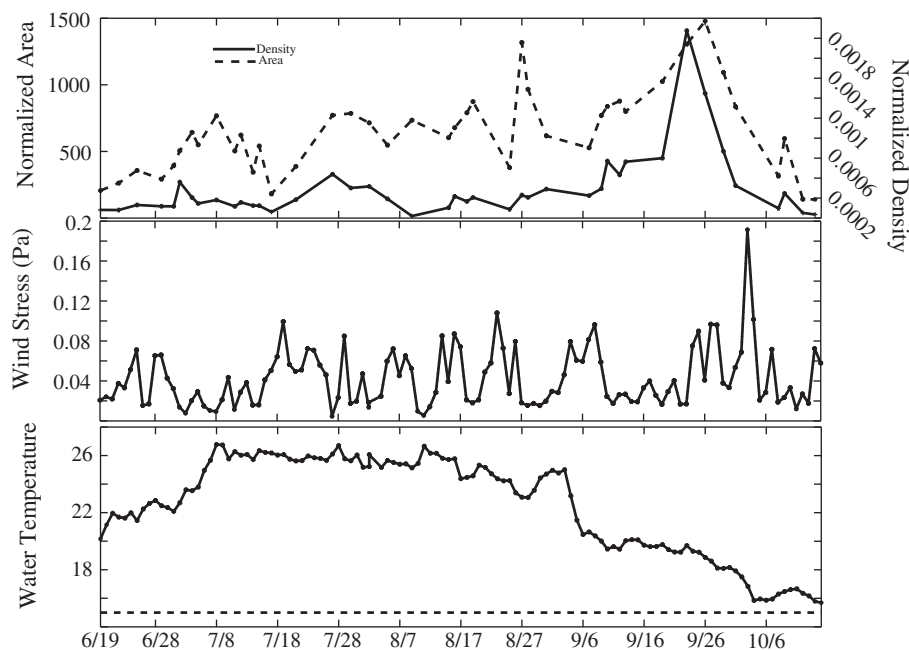


Fig. 8. Time series plots from 19 June to 14 October 2010. (A) Graph showing the normalized areal coverage of the bloom (dashed line) and the normalized density of the bloom (solid line). This data was extracted from the time series in Fig. 8. (B) Graph showing the mean daily wind stress from wind speed data reported by NOAA's NDBC station 45005. (C) Graph showing the mean daily water temperature as reported by NOAA's CO-OPS station at 45005. The dashed line shows the 15 °C point mentioned in the text.

Distribution of bulletin

Following the original design proposed by Stumpf et al. (2003), in 2008 the forecasts were emailed to a specific list of end users, which included local environmental and public health officials, natural resource managers, and drinking water utility managers via a pdf document. This has been shown to be the quickest and cheapest way to disseminate the forecasts to a user base. This specific group of subscribers also provided feedback on the accuracy of the forecasts in predicting blooms in Lake Erie. Stakeholder workshops were conducted in 2009 and 2010 to obtain additional information from end users on the layout and information provided from the forecasts and the feedback received was incorporated into later iterations of the forecasts. In 2010, distribution of the forecast HAB bulletin was switched to a web-based campaign of the pdf file, posted online weekly at: http://www.glerl.noaa.gov/res/Centers/HABS/lake_erie_hab/lake_erie_hab.html. The web based campaign has broadened distribution, enables subscribers to provide feedback on accuracy of the forecast, and provides tracking data to determine number of subscribers opening the HAB bulletin and forwarding it to others. From 2008 to 2011 distribution of the Lake Erie HAB bulletin has increased from 39 to over 180 subscribers (Table 1). As of this writing (well into the 2011 bloom season, the subscriber list has further increased to over 360). Several of the recipients of the forecasts are not located near Lake Erie but have expressed interest in having these types of forecasts available for the other Laurentian Great Lakes.

Table 1

Data on the number of HAB forecast bulletins issued each year and the number of subscribers that received those bulletins.

Year	Forecasts made	Number of subscribers
2008	6	39
2009	13	57
2010	20	183

Conclusions and recommendations

The work presented here has grown and expanded from the first generation of NOAA's Harmful Algal Bloom Forecasting System, which has been run operationally in Florida since 2004. The same framework has been incorporated with a more advanced hydrodynamic modeling/simulation component added. There is still room for improvements and developments within the context of the system. Modeling the vertical mixing would improve analysis of the imagery, particularly in assessing the recurrence of high surface biomass after a wind event. Such applications are being examined (Lanerolle et al., 2011). While a three-dimensional hydrodynamic model incorporated into similar particle tracking techniques described here may provide a more comprehensive examination of vertical distributions, initialization of the bloom field in three dimensions would be problematic, and would have to be assessed against forecast skill.

The available satellite time series could also be used to better understand the ecology of HAB blooms in western Lake Erie. Analysis of imagery data from previous years could provide information on the timing and intensity of bloom initiation, and decline which could then be assessed in light of data on river outflow, climatologic variables, nutrient variations, etc. to provide greater insight into the factors affecting phytoplankton composition and bloom dynamics within the basin of western Lake Erie.

The forecasts described here will continue to be disseminated for the foreseeable future and advances in the forecasting techniques will be made when possible. It is clear from the significant increase in number of subscribers that there is a growing interest in the product being generated and suggests that this HAB forecast product can meet a critical need of the scientific and management communities serving Lake Erie.

The ESA L2 products provided good discrimination of clouds and glint, but a real-time implementation of these has not yet been practical. Turning off the cloud mask had meant a high rate of false negative (blooms cannot be observed under clouds), but the new cloud mask being applied to the NASA I2gen products appears to produce comparable discrimination. The use of the I2gen surface reflectance

may offer greater flexibility as it will be consistent across the scene, even in high glint high reflectance water.

An additional improvement would be to devise a method to fill in missing data. If the initial image was contaminated with a cloud, there would not be any feature to model through time to create a nowcast or forecast for that particular time and location. Hence not only would the image be missing information, but the nowcast and the forecast would be misrepresentations of the actual bloom. There are a few separate techniques being considered on how best to do this. One of the most promising techniques uses a set of Empirical Orthogonal Functions (EOFs) in a software package called DINEOF (Alvera-Azcárate et al., 2005; Beckers and Rixen, 2003). DINEOF would require a few scenes prior to an image with missing or gappy data. The software uses EOFs to reconstruct what a feature would look like using previous data.

Supplementary data to this article can be found online at <http://dx.doi.org/10.1016/j.jglr.2012.10.003>.

Acknowledgements

MERIS imagery was provided by the European Space Agency (Category-1 Proposal C1P.9975). Funding was provided by the National Oceanic and Atmospheric Administration's (NOAA) Center of Excellence for Great Lakes and Human Health, the National Center for Environmental Health at the Centers for Disease Control and Prevention and the NASA Applied Science Program announcement NNH08ZDA001N under contract NNH09AL53I. The authors would like to thank Phil Keegstra and Lita Katz for assistance in processing data. The authors would like to thank Tom Bridgeman for invaluable communication throughout the years.

References

- Alvera-Azcárate, A., Barth, A., Rixen, M., Beckers, J.M., 2005. Reconstruction of incomplete oceanographic data sets using Empirical Orthogonal Functions. Application to the Adriatic Sea. *Ocean Model.* 9, 325–346.
- Beckers, J.M., Rixen, M., 2003. EOF calculations and data filling from incomplete oceanographic data sets. *J. Atmos. Oceanic Technol.* 20 (12), 1839–1856.
- Budd, J.W., Drummer, T.D., Nalepa, T.F., Fahnenstiel, G.L., 2001. Remote sensing of biotic effects: Zebra mussels (*Dreissena polymorpha*) influence on water clarity in Saginaw Bay, Lake Huron. *Limnol. Oceanogr.* 46, 213–223.
- ESA, 2012. Earthnet Online. <https://earth.esa.int/web/guest/missions/esa-operational-eo-missions/envisat/instruments/meris>.
- Fahnenstiel, G.L., Millie, D.F., Dyble, J., Litaker, R.W., Tester, P.A., McCormick, J., Rediske, R., Klarer, D., 2008. Factors affecting microcystin concentration and cell quota in Saginaw Bay, Lake Huron. *Aquat. Ecosyst. Health Manag.* 11, 190–195.
- Falconer, I.R., 2005. Is there a human health hazard from microcystins in the drinking water supply? *Acta Hydroch. Hydrob.* 33, 64–71.
- Fisher, K.M., Allen, A.L., Keller, H.M., Bronder, Z.E., Fenstermacher, L.E., Vincent, M.S., 2006. Annual report of the Gulf of Mexico Harmful Algal Bloom Operational Forecast System (GOM HAB-OFS). NOAA Tech. Rep. NOS CO-OPS 047.
- Fleming, L.E., Backer, L.C., Rowan, A., 2002. The epidemiology of human illness associated with harmful algal blooms. In: Baden, D., Adams, D. (Eds.), *Neurotoxicology Handbook*, 1. Humana Press Inc., Totowa, NJ, pp. 363–381.
- Graham, J.L., Loftin, K.A., Kamman, N., 2009. Monitoring recreational freshwaters. *Lakelines* 29, 18–24.
- Hsu, S.A., 1973. Experimental Results of the Drag-Coefficient Estimation for Air-Coast Interfaces. *Boundary-Layer Meteorology* 6, 505–507.
- Hunter, P.D., Tyler, A.N., Gilvear, D.J., Willby, N.J., 2008. The spatial dynamics of vertical migration by *Microcystis aeruginosa* in a eutrophic shallow lake: a case-study using high spatial resolution time-series airborne remote sensing. *Limnol. Oceanogr.* 53 (6), 2391–2406.
- Ibelings, B.W., Vonk, M., Los, H.F.J., Van der Molen, D.T., Mooij, W.M., 2003. Fuzzy modeling of cyanobacterial surface waterblooms: validation with NOAA-AVHRR satellite images. *Ecol. Appl.* 13, 1456–1472.
- Juhel, G., Davenport, J., O'Halloran, J., Culloty, S., Ramsey, R., James, K., Furey, A., Allis, O., 2006. Pseudodiarthra in zebra mussels *Dreissena polymorpha* (Pallas) exposed to microcystins. *J. Exp. Biol.* 209, 810–816.
- Lanerolle, L.W.J., Stumpf, R.P., Wynne, T.T., Patchen, R.C., 2011. A one-dimensional numerical vertical mixing model with application to western Lake Erie. NOAA Technical Memorandum NOAA NCCOS 131. National Oceanic and Atmospheric Administration, National Ocean Service, National Centers for Coastal Ocean Science. (Silver Spring, MD. 44 pp.).
- Makarewicz, J.C., 1993. Phytoplankton biomass and species composition in Lake Erie, 1970 to 1987. *J. Great Lakes Res.* 19, 258–274.
- Montagner, F., 2001. Reference model for MERIS level 2 processing. European Space Agency, document PO-TN-MEL-GS-0026.
- NASA, 2011. L2gen Users' Guide. <http://oceancolor.gsfc.nasa.gov/DOCS/MSL12/>.
- Nicholls, K., Hopkins, G.J., 1993. Recent changes in Lake Erie (north shore) phytoplankton: cumulative impacts of phosphorus loading reduction and the zebra mussel introduction. *J. Great Lakes Res.* 19, 637–647.
- NOAA, 2008. NOAA Administrative Order 216-105. http://www.corporateservices.noaa.gov/%7Eames/NAOs/Chap_216/naos_216_105.html.
- Paerl, H.W., 1988. Nuisance phytoplankton blooms in coastal, estuarine, and inland waters. *Limnol. Oceanogr.* 33, 823–847.
- Paerl, H.W., Huisman, J., 2008. Blooms like it hot. *Science* 320, 57–58.
- Paerl, H.W., Fulton, R.S., Moisan, P.H., Dyble, J., 2001. Harmful freshwater algal blooms, with an emphasis on cyanobacteria. *Sci. World* 1, 76–113.
- Rast, M., Bezy, J.L., Bruzzi, S., 1999. The ESA Medium Resolution Imaging Spectrometer MERIS—a review of the instrument and its mission. *Int. J. Remote. Sens.* 20, 1681–1702.
- Richardson, K., 1989. Algal blooms in the North Sea: the good, the bad, and the ugly. *Dana* 8, 83–93.
- Rinta-Kanto, J.M., Ouellette, A.J.A., Boyer, G.L., Twiss, M.R., Bridgeman, T.B., Wilhelm, S.W., 2005. Quantification of Toxic Microcystis spp. during the 2003 and 2004 Blooms in Western Lake Erie using Quantitative Real-Time PCR. *Environ. Sci. Technol.* 39, 4198–4205.
- Schwab, D.J., Bedford, K.W., 1999. The Great Lakes Forecasting System. In: Mooers, C.N.K. (Ed.), *Coastal Ocean Prediction, Coastal and Estuarine Studies* 56. American Geophysical Union, Washington, DC, pp. 157–173.
- Sellner, K.G., 1997. Physiology, ecology, and toxic properties of marine cyanobacteria blooms. *Limnol. Oceanogr.* 42, 1089–1104.
- Smayda, T.J., 1997. What is a bloom? A commentary. *Limnol. Oceanogr.* 42 (5, pt. 2), 1132–1136.
- Stumpf, R.P., Culver, M.E., Tester, P.A., Tomlinson, M., Kirkpatrick, G.J., Pederson, B.A., Truby, E., Ransibrahmanakul, V., Soracco, M., 2003. Monitoring *Karenia brevis* blooms in the Gulf of Mexico using satellite ocean color imagery and other data. *Harmful Algae* 2, 147–160.
- Stumpf, R.P., Tomlinson, M.C., Calkins, J.A., Kirkpatrick, B., Fisher, K., Nierenberg, K., Currier, R., Wynne, T.T., 2009. Skill assessment for an operational algal bloom forecast system. *J. Mar. Syst.* 76, 151–161.
- Tomlinson, M.C., Stumpf, R.P., Ransibrahmanakul, V., Truby, E.W., Kirkpatrick, G.J., Pederson, B.A., Vargo, G.A., Heil, C.A., 2004. Evaluation of the use of SeaWiFS imagery for detecting *Karenia brevis* harmful algal blooms in the eastern Gulf of Mexico. *Remote. Sens. Environ.* 91 (3–4), 293–303.
- Vanderploeg, H.A., Liebig, J.R., Carmichael, W.W., Agy, M.A., Johengen, T.H., Fahnenstiel, G.L., Nalepa, T.F., 2001. Zebra mussel (*Dreissena polymorpha*) selective filtration promoted toxic Microcystis blooms in Saginaw Bay (Lake Huron) and Lake Erie. *Can. J. Fish. Aquat. Sci.* 58, 1208–1221.
- World Health Organization, 2003. Guidelines for safe recreational water environments. Coastal and fresh waters, volume 1. Geneva, Switzerland. (220 pp.).
- Wynne, T.T., Stumpf, R.P., Tomlinson, M.C., Ransibrahmanakul, V., Villareal, T.A., 2005. Detecting *Karenia brevis* blooms and algal resuspension in the western Gulf of Mexico with satellite ocean color imagery. *Harmful Algae* 4 (6), 992–1003.
- Wynne, T.T., Stumpf, R.P., Tomlinson, M.C., Warner, R.A., Tester, P.A., Dyble, J., Fahnenstiel, G.L., 2008. Relating spectral shape to cyanobacterial blooms in the Laurentian Great Lakes. *Int. J. Remote. Sens.* 29 (12), 3665–3672.
- Wynne, T.T., Stumpf, R.P., Tomlinson, M.C., Dyble, J., 2010. Characterizing a cyanobacterial in western Lake Erie using satellite imagery and meteorologic data. *Limnol. Oceanogr.* 55 (5), 2025–2036.
- Wynne, T.T., Stumpf, R.P., Tomlinson, M.C., Schwab, D.J., Watabayashi, G.Y., Christensen, J.D., 2011. Estimating cyanobacterial bloom transport by coupling remotely sensed imagery and a hydrodynamic model. *Ecol. Appl.* 21 (7), 2709–2721.